

pH-Sensitive and Thermosensitive Hydrogels as Stem-Cell Carriers for Cardiac Therapy

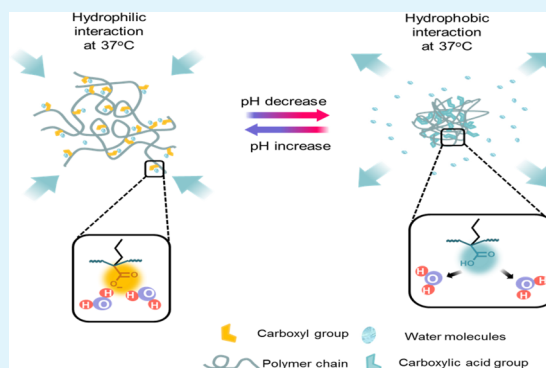
Zhenqing Li,^{†,‡} Zhaobo Fan,^{†,‡} Yanyi Xu,^{†,‡} Wilson Lo,[†] Xi Wang,[†] Hong Niu,[†] Xiaofei Li,[†] Xiaoyun Xie,[§] Mahmood Khan,[‡] and Jianjun Guan^{*,†,||}

[†]Department of Materials Science and Engineering and [‡]Department of Emergency Medicine, Davis Heart Lung Research Institute, The Ohio State University, Columbus, Ohio 43210, United States

[§]Department of Gerontology, Tongji Hospital, and ^{||}Tongji Hospital, Tongji University, Shanghai, China

ABSTRACT: Stem-cell therapy has the potential to regenerate damaged heart tissue after a heart attack. Injectable hydrogels may be used as stem-cell carriers to improve cell retention in the heart tissue. However, current hydrogels are not ideal to serve as cell carriers because most of them block blood vessels after solidification. In addition, these hydrogels have a relatively slow gelation rate (typically >60 s), which does not allow them to quickly solidify upon injection, so as to efficiently hold cells in the heart tissue. As a result, the hydrogels and cells are squeezed out of the tissue, leading to low cell retention. To address these issues, we have developed hydrogels that can quickly solidify at the pH of an infarcted heart (6–7) at 37 °C but cannot solidify at the pH of blood (7.4) at 37 °C. These hydrogels are also clinically attractive because they can be injected through catheters commonly used for minimally invasive surgeries. The hydrogels were synthesized by free-radical polymerization of *N*-isopropylacrylamide, propylacrylic acid, hydroxyethyl methacrylate-*co*-oligo(trimethylene carbonate), and methacrylate poly(ethylene oxide) methoxy ester. Hydrogel solutions were injectable through 0.2-mm-diameter catheters at pH 8.0 at 37 °C, and they can quickly form solid gels under pH 6.5 at 37 °C. All of the hydrogels showed pH-dependent degradation and mechanical properties with less mass loss and greater complex shear modulus at pH 6.5 than at pH 7.4. When cardiosphere-derived cells (CDCs) were encapsulated in the hydrogels, the cells were able to survive during a 7-day culture period. The surviving cells were differentiated into cardiac cells, as evidenced by the expression of cardiac markers at both the gene and protein levels, such as cardiac troponin T, myosin heavy chain α , calcium channel CACNA1c, cardiac troponin I, and connexin 43. The gel integrity was found to largely affect CDC cardiac differentiation. These results suggest that the developed dual-sensitive hydrogels may be promising carriers for cardiac cell therapy.

KEYWORDS: thermosensitive hydrogel, pH-sensitive hydrogel, catheter delivery, cardiosphere-derived cells, cardiac differentiation



1. INTRODUCTION

Cardiovascular disease is the leading cause of death in the United States. Myocardial infarction (MI) is one of the major cardiovascular diseases. Currently, coronary artery bypass surgery (CABG) and percutaneous coronary intervention (PCI) are used to reestablish the blood flow to the infarcted areas. In PCI, a catheter was used in balloon-based angioplasty and the placement of a stent. The advantage of PCI lies in its minimally invasive strategy. However, the possibility of vessel wall damage during PCI raises the high risk of thrombogenesis.¹ Another drawback of PCI is its low efficacy in revascularization of infarcted areas compared to CABG.² The delivery of anticoagulation drugs and vascularization growth factors during PCI is a possible solution because they can suppress thrombogenesis and stimulate angiogenesis, respectively. Currently, delivery vehicles of these drugs or biomolecules include drug-eluting stents,³ polymer microspheres,⁴ and hydrogels.^{5,6}

Nevertheless, neither CABG nor PCI strategies can regenerate new cardiomyocytes to compensate for cell loss after MI. The delivery of stem cells is considered to be a promising solution. Many types of stem cells have been used in cardiac cell therapy, including mesenchymal stem cells,^{7,8} skeleton muscle stem cells,⁹ embryonic stem-cell-derived cardiomyocytes,^{10,11} induced pluripotent stem cells,¹² and cardiosphere-derived cells (CDCs).^{13–15} CDCs are derived from endocardium biopsy and have a fast proliferation rate when cultured *ex vivo*. They can differentiate into endothelial cells, cardiac myocytes, and smooth muscle cells.¹³ Therefore, CDCs are considered to be one of the promising autologous adult progenitor cells for cardiac cell therapy.

Direct injection of stem cells into the infarcted area results in low cell retention and poor long-term engraftment.^{16–18} This is

Received: February 9, 2016

Accepted: April 11, 2016

Published: April 11, 2016

mainly due to the cellular apoptosis induced by the local harsh ischemic environment and lack of cell anchorage for survival. In our previous work, thermosensitive hydrogels loaded with antioxidant drugs,¹⁹ angiogenic growth factors,^{20,21} or oxygen release microspheres²² were used to address these issues. The results showed that cell survival was significantly improved under the low oxygen/low nutrient conditions or high reactive oxygen species environment. However, gels developed in these reports cannot be directly used for catheter-based PCI delivery because they are thermosensitive only and may block the catheter during the injection.

Hydrogels used for catheter delivery include polyelectrolyte pullulan,⁵ in situ gelling fibrin glue,⁶ shape-defined alginate hydrogel,²³ thermosensitive triblock copolymer poly(ethylene glycol) (PEG)–poly(lactic acid) (PLA)–PEG,²⁴ collagen gel,²⁵ and pH-sensitive hydrogels like sulfamethazine oligomer-terminated polycaprolactone (PCLA)–PEG–PCLA.²⁶ The infarcted area has a lower local pH than normal cardiac tissues because of the inflammation induced by acute MI.^{27,28} Therefore, a hydrogel that is responsive to the pH difference is suitable for catheter-based delivery.

Many polymers are introduced as potential pH-sensitive hydrogel candidates for biomedical applications. Natural pH-sensitive hydrogels, like collagen and chitosan, are soluble at acidic pH but form gels at neutral pH.²⁹ Synthetic polymers provide wider prospects of pH sensitivity, with a pH-responsive range between 3 and 10.³⁰ Poly(acrylic acid),^{31,32} poly(methacrylic acid),³³ and sulfonamide-based polymers³⁴ solidify at acidic pH, while basic pH-responsive polymers including poly(amino ester),^{35,36} poly(*tert*-amine methacrylate)^{37,38} and poly(2-vinylpyridine)³⁹ can form gels at basic pH. To use a catheter to deliver hydrogels into infarcted hearts, the hydrogels should be acid-pH-responsive because the infarcted area has a lower pH than that of the normal tissue. Most acid-pH-responsive hydrogels are based on acrylic acid and methacrylic acid that have pH (2–4.5) values far lower than that of the infarcted tissue (6–7).^{27,28} Murthy et al. found that the incorporation of propylacrylic acid (PAA; $pK_a \sim 6.3$) into hydrogels allowed a pH-responsive range between 6 and 7.⁴⁰ The synthesized thermosensitive and pH-sensitive poly(*N*-isopropylacrylamide-*co*-propylacrylic acid-*co*-butyl acrylate) (PNIPAAm–PAA–BA) was used as a drug carrier for a basic fibroblast growth factor.^{41,42} However, the nondegradable nature of PNIPAAm–PAA–BA may be a limitation in cell-based therapy.

In this work, a family of PAA-based degradable and thermosensitive and pH-sensitive hydrogels were synthesized by copolymerizing NIPAAm, PAA, methacrylate poly(ethylene glycol) methyl ether (MA-PEG), and biodegradable macromer 2-hydroxyethyl methacrylate-*co*-oligo(trimethylene carbonate) (HEMA-*o*TMC) (Figure 1). The hydrogel injectability and thermal, mechanical, and degradation properties were assessed under different pH values. Furthermore, CDCs were encapsulated in the hydrogels, and cell survival and cardiac differentiation were evaluated by real-time reverse transcription polymerase chain reaction (RT-PCR) and immunohistochemistry.

2. EXPERIMENTAL MATERIALS AND METHODS

2.1. Materials. Diethyl propylmalonate (99%), potassium hydroxide, and diethylamine (99%+) were purchased from Alfa Aesar and used without further purification. A formaldehyde solution (36.5–38.0%) was obtained from Mallinckrodt Chemicals and used as

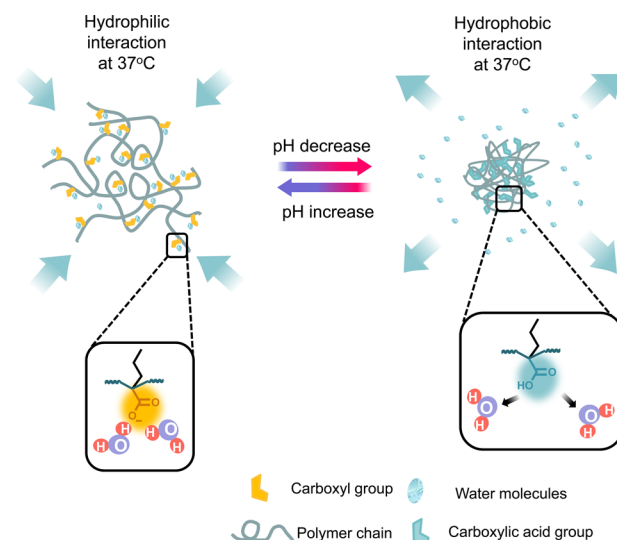


Figure 1. Design of the pH sensitivity in PNIPAAm-based thermosensitive hydrogels.

received. Concentrated sulfuric acid was purchased from Fisher and used directly. *N*-Isopropylacrylamide (NIPAAm), poly(ethylene glycol) methyl ether (MA-PEG), and 2-hydroxyethyl methacrylate (HEMA) were purchased from VWR. NIPAAm was recrystallized three times by hexane. MA-PEG and HEMA were purified by vacuum distillation. Trimethylene carbonate was obtained from Boehringer Ingelheim and used without further purification. All solvents were purchased from VWR and used as received.

2.2. Synthesis of PAA. PAA was synthesized following the methods in previous reports^{40,43} with modification (Figure 2). Briefly,

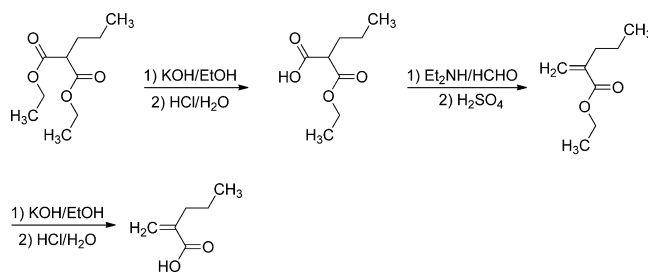


Figure 2. Synthesis of PAA.

50 g of diethyl propylmalonate was stirred in 350 mL of 1 mol/L KOH and a 95% ethanol solution overnight. The mixture was condensed by a rotary evaporator. Hydrochloric acid was further added to the yellowish oil, and the solution pH was adjusted to 1.5–2. A total of 600 mL of ethyl ether was used to extract the crude product. The ether layer was further dried by magnesium sulfate overnight and filtered. Excess ether was removed by a rotary evaporator. The oily product was further mixed with 27.5 mL of diethylamine at 0 °C. After mixing, 21.8 mL of a formaldehyde solution was slowly added by an addition funnel. Following stirring overnight, the addition funnel was replaced by a condenser. The mixture was heated to 60 °C and stirred for another 12 h. The mixture was then cooled to 0 °C with the addition of sulfuric acid. Ether was further used to extract the product. The structure of crude ethyl 2-propylacrylate was verified by ¹H NMR. It was further hydrolyzed by 1 mol/L KOH and refluxed under 60 °C. Hydrochloric acid was used to adjust the pH to 1.5–2. A yellow oil-like crude product was separated and further extracted by diethyl ether. The final product was obtained by removing the ether with a rotary evaporator. The structure of the final PAA was verified by ¹H NMR (Figure 3): δ 6.28 (1H, s, CH₂=), 5.64 (1H, s, CH₂=), 2.28 (2H, t, –CH₂–), 1.49 (2H, m, –CH₂–), 0.92 (3H, m, CH₃–).

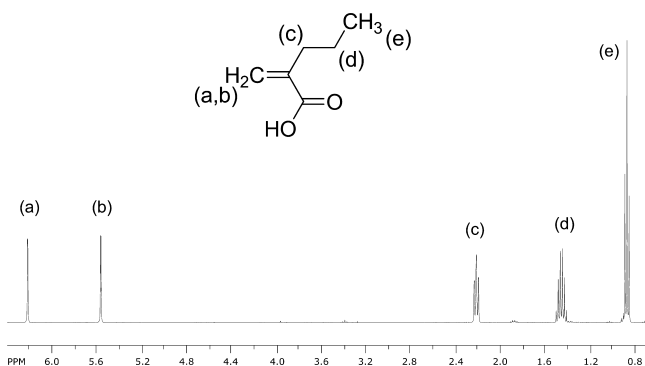


Figure 3. ^1H NMR spectrum of PAA.

2.3. Synthesis of Poly(NIPAAm-co-PAA-co-HEMA-oTMC-co-MA-PEG). HEMA-oTMC was synthesized based on previously reported methods.^{19,43} The obtained HEMA-oTMC had an average of 2.2 TMC units calculated from the ^1H NMR spectrum. Poly(NIPAAm-co-PAA-co-HEMA-oTMC-co-MA-PEG) was synthesized via free-radical polymerization of NIPAAm, PAA, HEMA-oTMC, and MA-PEG (Figure 4). The monomers and macromer were dissolved in dioxane and charged in a 250 mL round-bottom flask. Benzoyl peroxide was used as an initiator. The reaction was conducted at 60 °C overnight under the protection of nitrogen. The polymer was precipitated by hexane, purified by tetrahydrofuran (THF)/ethyl ether twice, and dried under vacuum.

2.4. Characterization of Synthesized Hydrogels. The structures of the copolymers were characterized by ^1H NMR. The composition was determined by the ratio between the integration of characteristic peaks of different functional groups. The molecular weights and polydispersity indexes (PDIs) of the copolymers were determined by gel permeation chromatography (GPC). THF and polystyrene were used as the solvent and standard, respectively. The hydrogel solutions were prepared by dissolving copolymers in Dubecco's modified phosphate-buffered saline (DPBS). The final concentration was 20 wt %. The injectability of the hydrogel solutions was tested by injecting the prewarmed solutions (37 °C) through a

catheter (Abbott Voyage, inner diameter 0.2 mm) to 37 °C sodium phosphate buffers with pH values of 6.5 and 7.4. The catheter was immersed in a 37 °C water bath. The lower critical solution temperatures (LCSTs) of the solutions at pH values of 6.5, 7.4, and 8.0 were measured by differential scanning calorimetry (DSC) using thermal scanning from 0 to 60 °C with a 10 °C/min increment. The temperature at the maximum endothermic peak was considered to be the LCST.

Solid gels were formed by incubating the hydrogel solutions in a pH 6.5 buffer at 37 °C. To determine the pH responsiveness, hydrogels were equilibrated under a sodium phosphate buffer of either pH 6.5 or 7.4 for 24 h. The rationale of using a sodium phosphate buffer was to test the gel response under different pH values without changing the ionic strength. For mechanical testing, hydrogels were placed in a cone-plate rheometer equipped with a temperature-controlled Peltier and a cap to prevent evaporation. The gap distance was set as the thickness of the gels. A strain sweep (0.1–3%) with a 1 Hz frequency was used. A further frequency sweep from 1 to 10 Hz with strain in the linear viscoelastic region was applied. The storage, loss modulus, and complex viscosity were recorded. Afterward, a large strain sweep from 0.1% to 15% was further used.

The hydrogel water content was determined based on the wet weight of the hydrogel w_1 and the lyophilized weight w_2 . The water content was calculated as

$$\text{water content (\%)} = (w_1 - w_2)/w_2 \times 100\%$$

Hydrogel degradation was conducted in pH 6.5 and 7.4 buffers to investigate the effect of the pH on the degradation rate. The solid hydrogels were placed in 2 mL microcentrifuge tubes containing 1.5 mL of a prewarmed buffer. Degradation was conducted in a 37 °C water bath. The samples were taken at defined intervals and freeze-dried before being weighed (w_3). The weight loss was calculated as

$$\text{weight remaining (\%)} = w_3/w_4 \times 100\%$$

where w_4 is the sample weight before degradation.

2.5. Encapsulation of CDCs in Hydrogels. Murine CDCs were cultured by using an Iscove modified Dubecco's medium (IMDM) supplemented with 10% fetal bovine serum, 2% L-glutamine, and 1% antibiotics. The medium was changed every 3 days. Cells were

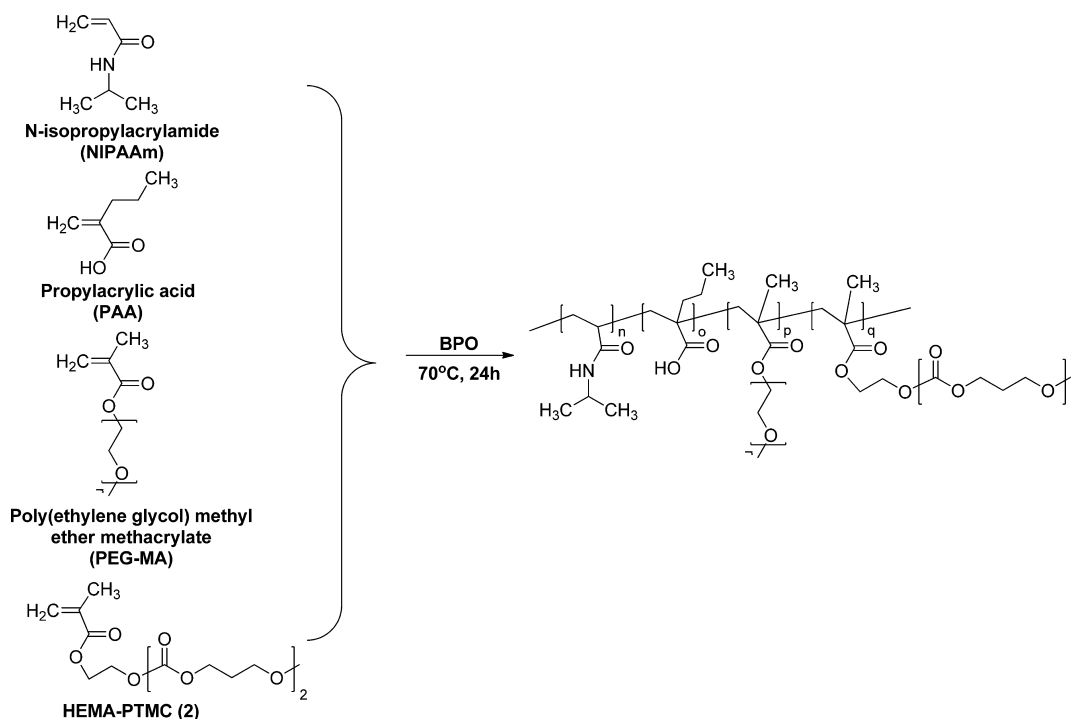


Figure 4. Synthesis scheme of poly(NIPAAm-co-PAA-co-MA-PEG-co-HEMA-oTMC).

Table 1. Primers Used for Real-Time RT-PCR

name	forward (5'-3')	reverse (5'-3')	T _m (Fwd/Rev, °C)	product size (bp)
β -actin	AAGATCAAGATCATTGCTCCTC	GGACTCATCGTACTCCTG	61.2/59.5	110
cTnT	TACATCCAGAAGACAGAGCG	CTCTCAGTTGGTCTTCATTACAG	61.4/60.7	123
MYH6	GAGGAGATGCGAGATGAGAG	CGGTTTGTCTTGAAGTAGAGC	61.6/61.3	194
CACNA1c	TCTCATCTGCTCAACACCA	ATCACAGAAATAGTGCTTGGGT	61.3/60.2	162

passed when 90% confluence was reached. CDCs of passages 11–14 were used. A CDC suspension with a density of 20 million/mL was prepared by trypsinizing and resuspending cells in DPBS. A total of 0.5 mL of the cell suspension was added into 1 mL of a hydrogel solution at 4 °C and mixed thoroughly. Hydrogel/cell constructs were then formed by incubating the mixture at 37 °C for 20–30 min. The supernatant was replaced by an equal amount of the cell culture medium (pH 7.4).

2.6. Survival and Cardiac Differentiation of CDCs in Hydrogels. To assess cell survival, cell/hydrogel constructs were collected after 1 and 7 days of culture, followed by digestion in a papain solution at 60 °C. The double-stranded DNA (dsDNA) content in the solution was quantified by PicoGreen assay (Invitrogen). To assess cardiac differentiation of the encapsulated CDCs at the gene level, cell/hydrogel constructs were first immersed in TRIzol (Sigma) to isolate the total RNA following the manufacturer's protocol. The quality of RNA was monitored by a Nanodrop system. A total of 1 μ g of RNA was utilized to synthesize cDNA. Primers of forward and reverse pairs of cardiac troponin T (cTnT), myosin heavy chain α (MYH6), and calcium channel, voltage-dependent, L type, α 1c (CACNA1c), and β -actin were designed using *PerilPrimer* software. The sequences and melting temperatures are listed in Table 1. Real-time RT-PCR was conducted in triplicate for each sample with a Maxima SYBR Green/fluorescein master mix on an Applied Biosystem 7900 system. β -Actin was used as the housekeeping gene. Fold differences were calculated using a standard $\Delta\Delta$ Ct method.

To assess CDC cardiac differentiation at the protein level, cell/hydrogel constructs were taken after 7 days of culture and fixed in 4% paraformaldehyde for 1 h. The constructs were further embedded in an optimal cutting temperature solution and sectioned at -20 °C with a thickness of 10 μ m. The sections were blocked by 10% goat serum, permeabilized by 0.3% Triton X-100 for 1 h, incubated with primary antibodies mouse antimouse cardiac troponin I (cTnI; Abcam) and rabbit antimouse connexin 43 (CX43) at 37 °C overnight, and finally incubated with secondary antibodies Dylight488 conjugated goat antimouse IgG and AlexaFluo647 conjugated goat antirabbit IgG (Jackson Immuno) at 37 °C for 1 h. Hoechst 33342 was used to counterstain the nucleus. Sections without primary antibody incubation were treated as negative controls. All images were observed under an Olympus FV1000 confocal microscope.

2.7. Statistical Analysis. Data are reported as mean \pm standard deviation. Multivariate repeated-measures ANOVA were used to compute the statistical significance between different groups. A statistical significance was considered when $p < 0.05$.

3. RESULTS

3.1. Synthesis of Poly(NIPAAm-co-PAA-co-MA-PEG-co-HEMA-oTMC). Poly(NIPAAm-co-PAA-co-MA-PEG-co-HEMA-oTMC) was synthesized by free-radical polymerization of NIPAAm, PAA, MA-PEG, and HEMA-oTMC. The structures of the copolymers were validated by ¹H NMR (Figure 5). In a typical ¹H NMR spectrum, all of the characteristic peaks for NIPAAm (b), PAA (a'), MA-PEG (c and d), and HEMA-oTMC (g, h, i, j, k, and k') appeared. The copolymer composition was determined by the ratio between integrations of these peaks and is listed in Table 2. The compositional ratio of the copolymers was found to be consistent with the feed ratio. The three copolymers had molecular weights of 9.2–11.0 kDa and PDIs of 1.2–1.4. The

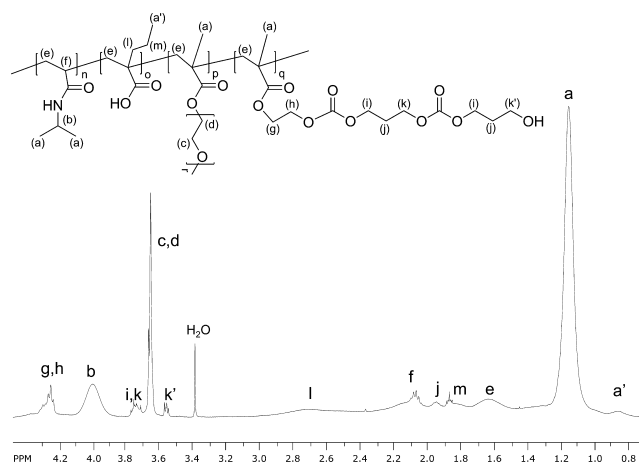


Figure 5. ¹H NMR spectrum of poly(NIPAAm-co-PAA-co-MA-PEG-co-HEMA-oTMC).

Table 2. Copolymer Feed Ratio, Composition, Molecular Weight, and PDI

gel	feed ratio ^a	composition ^a	M _n	PDI
EG1	87/6/5/2	87/5.3/4.8/2.9	9591	1.3
EG2	86/6/5/3	86/5.2/4.3/4.5	9234	1.2
EG3	84/6/7/3	84/5.5/6.3/4.2	10956	1.4

^aRatio of NIPAAm/PAA/HEMA-oTMC/MA-PEG.

relatively low molecular weights may be due to the usage of a polystyrene standard during GPC tests because its molecular structure is largely different from the synthesized copolymers.

3.2. Hydrogel Solution Injectability, Gelation, and LCST at Different pH Values. The synthesized copolymers were able to dissolve in DPBS to form 20 wt % hydrogel solutions. All of the solutions were injectable through a 0.2-mm-diameter catheter at 37 °C when the pH was adjusted to 8.0. The gelation of the hydrogel solutions was pH-dependent. When the pH 8.0 solution was injected into the 37 °C buffer with a pH of 7.4, EG1 solidified and EG2 and EG3 retained a solution state. In contrast, all three solutions solidified upon injection into the 37 °C buffer with a pH of 6.5 (Figure 6).

To understand the pH-dependent gelation behavior of the hydrogels, LCSTs of the hydrogel solutions at different pH values were measured by DSC and are listed in Table 3. At pH 8.0, all three hydrogel solutions had LCSTs well above 37 °C, indicating that they cannot solidify but remain flowable at 37 °C. A substantial decrease in the LCST was observed for the hydrogel solutions when the pH was decreased from 8.0 to 7.4 and 6.5. For EG1, the LCSTs at pH 6.5 and 7.4 were lower than 37 °C, suggesting that it can solidify at both pH values. For EG2 and EG3, the LCSTs at pH 7.4 were greater than 37 °C, while at pH 6.5, they were lower than 37 °C. These two hydrogels can thus solidify at 37 °C when the pH is 6.5 instead of 7.4. The LCSTs of the hydrogels were also dependent on the composition. An increase in the ratio of the hydrophilic

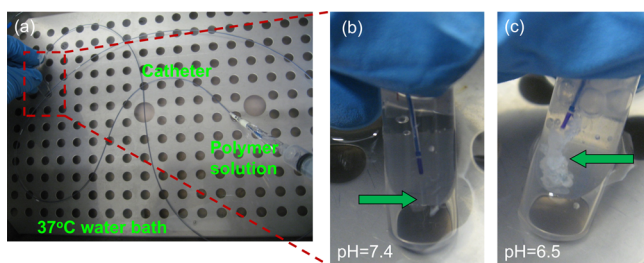


Figure 6. Injection of a hydrogel solution into a sodium phosphate buffer with different pH values through a catheter: (a) test setup (the temperature of the water bath was 37 °C); (b) injection of a 37 °C hydrogel solution into a pH 7.4, 37 °C buffer; (c) injection of a 37 °C hydrogel solution into a pH 6.5, 37 °C buffer.

Table 3. Hydrogel LCST and Gelation Capability under Different pH Values

gel	LCST (°C)			gelation ^a		
	pH 6.5	pH 7.4	pH 8.0	pH 6.5	pH 7.4	pH 8.0
EG1	31.9 ± 0.9	35.9 ± 0.3	40.5 ± 0.6	+	+	-
EG2	33.6 ± 0.6	39.7 ± 0.4	41.6 ± 0.2	+	-	-
EG3	29.5 ± 0.4	38.4 ± 0.4	39.8 ± 0.2	+	-	-

^a+ = gelation; - = no gelation.

component MA-PEG increased the LCST (EG2 vs EG1). On the other hand, an increase in the ratio of the hydrophobic HEMA-*o*TMC component decreased the LCST (EG2 vs EG3).

3.3. Hydrogel Mechanical Properties at Different pH Values. The mechanical properties of the hydrogels formed at pH 6.5 were characterized using a rheometer. All of the hydrogels showed a typical shear-thinning behavior because the

complex shear moduli decreased with an increase of the shear rate. The hydrogels were highly soft with complex shear moduli at an initial 1 Hz and pH 6.5 ranging from 580 to 1418 Pa. The modulus was dependent on the hydrogel composition. An increase in the hydrophobic HEMA-*o*TMC content significantly increased the complex shear moduli ($p < 0.01$), while an increase in the hydrophilic MA-PEG content significantly decreased the complex shear moduli ($p < 0.01$).

To investigate whether the mechanical properties of the hydrogels formed at pH 6.5 varied in the pH 7.4 environment, the hydrogels were incubated in IMDM with a pH of 7.4. After 1 day, the complex shear moduli for EG2 and EG3 dropped dramatically. This is expected because their LCSTs were higher than 37 °C at pH 7.4 (Table 3).

3.4. Degradation of Hydrogels under Different pH Values. The degradation property of the hydrogels formed at pH 6.5 was investigated after incubation in the buffers with different pHs (Figure 7). All three hydrogels demonstrated a pH-dependent degradation behavior. At pH 6.5, the hydrogels did not show significant weight loss during the 14-day degradation period. For the same hydrogel, the weight remaining under pH 6.5 was significantly higher than that under pH 7.4, suggesting that the hydrogels degraded faster at pH 7.4. Besides mass change, hydrogel water contents also varied throughout the degradation process. After 14 days, the hydrogels degraded under pH 7.4 had significantly higher water contents than those degraded under pH 6.5 (Figure 7).

3.5. CDC Survival in Hydrogels. To examine the biocompatibility of the hydrogels, CDCs were encapsulated and cultured for 7 days. Cell survival was quantified by the dsDNA content (for live cells). Figure 8 demonstrated that the cells survived in all three hydrogels because the dsDNA content did not change during the culture ($p > 0.05$). These results

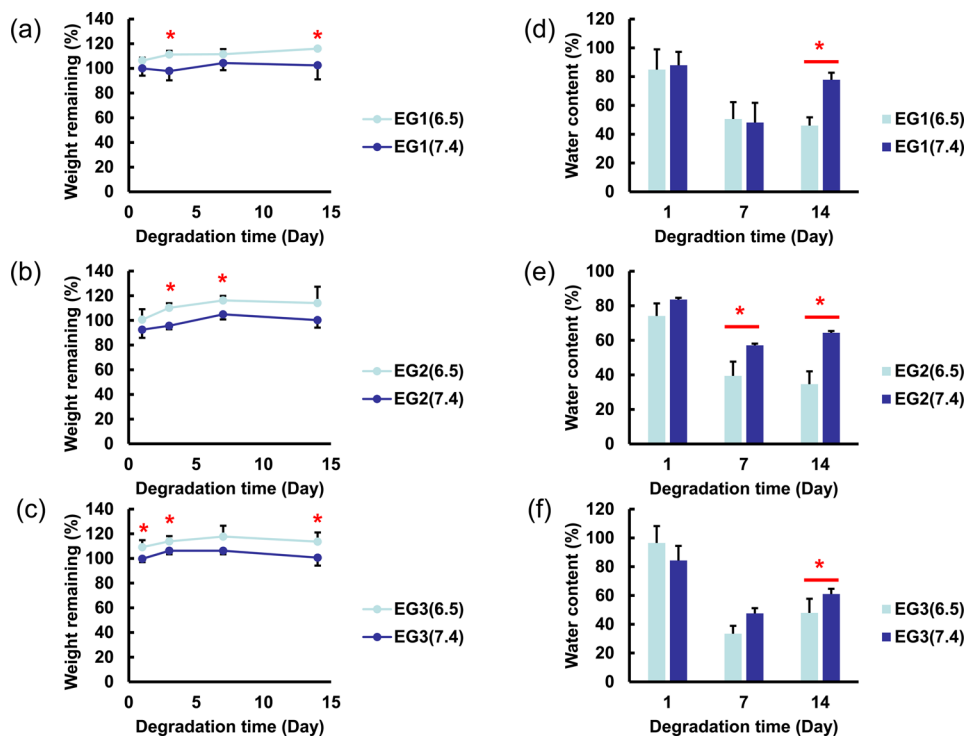


Figure 7. Degradation of EG1 (a), EG2 (b), and EG3 (c) in pH 6.5 and 7.4 buffers for 14 days and the water contents of the remaining EG1 (d), EG2 (e), and EG3 (f).

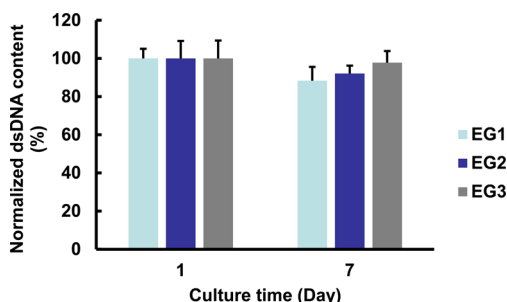


Figure 8. dsDNA contents of CDCs in the hydrogels after culture for 1 and 7 days.

were consistent with live cell staining, where the cell density did not vary substantially at days 1 and 7 (Figure 9).

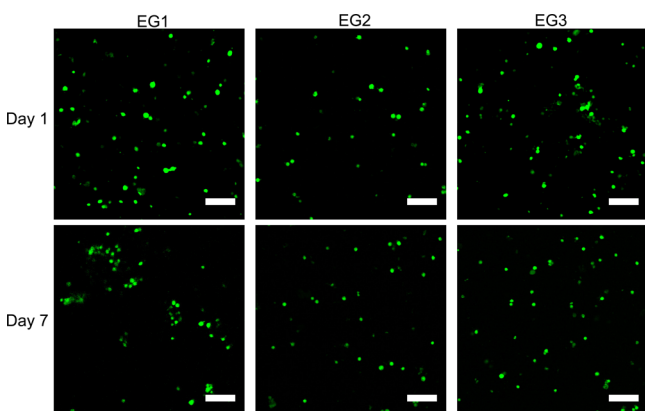


Figure 9. Live cell staining of CDCs cultured in hydrogels at days 1 and 7. The scale bars are 100 μm .

3.6. Cardiac Differentiation of CDCs in Hydrogels.

CDCs are capable of differentiating in cardiomyocytes in vitro and in vivo.^{13–15} To investigate whether CDCs encapsulated in

the hydrogels differentiated in cardiac lineage, cellular expressions of cardiac markers were characterized at both the gene and protein levels by real-time RT-PCR and immunohistochemical staining, respectively. At the mRNA level, the expressions of cTnT, MYH6, and CACNA1c were significantly upregulated for CDCs in EG1 and EG3 hydrogels compared to those in a 2D culture plate ($p < 0.05$; Figure 10). Meanwhile, CDCs in the EG1 hydrogel exhibited the highest expressions of cTnT, MYH6, and CACNA1c. Cardiac proteins including cTnI and gap junction protein CX43 were used to qualitatively detect cardiac differentiation at the protein level. CDCs in all three hydrogels exhibited cTnI expression. In contrast, more CDCs in the EG1 hydrogel than in the EG2 and EG3 hydrogels expressed CX43 (Figure 11).

4. DISCUSSION

In this report, a family of injectable hydrogels with the ability to respond to both the pH and temperature were synthesized. Hydrogel properties like the LCST, dynamic mechanical properties, degradation rate, and water content were pH-dependent. The hydrogels had good biocompatibility and were able to drive the encapsulated CDCs to differentiate the cardiac lineage.

4.1. Synthesis of Dual pH-Sensitive and Thermosensitive Hydrogels. In the synthesized hydrogels, the PAA and NIPAAm components were used to introduce the pH and thermal sensitivity, respectively. PAA allowed the hydrogels to have LCSTs higher than 37 $^{\circ}\text{C}$ at pH 8.0. Therefore, these hydrogels were able to remain flowable and injectable at 37 $^{\circ}\text{C}$. PAA also allowed the hydrogels to have LCSTs lower than 37 $^{\circ}\text{C}$ at pH 6.5 so as to form solid gels at this pH (Table 3). Because infarcted hearts typically exhibit pH values in the range of 6–7,^{27,28} the synthesized hydrogels should be able to solidify after injection into the infarcted area. PAA belongs to an alkylacrylic acid group, which has been used as an active compound to develop pH-sensitive polymers. The pK_a values of these acrylic acids typically increase when the length of the alkyl

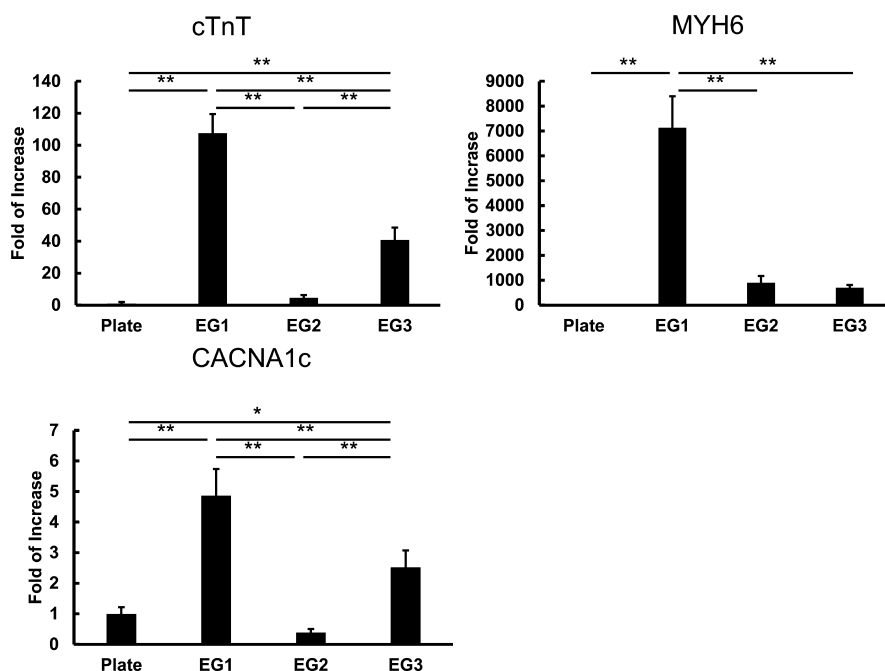


Figure 10. Quantification of the cardiac markers for CDCs cultured in hydrogels by real-time RT-PCR: *, $p < 0.05$; **, $p < 0.01$.

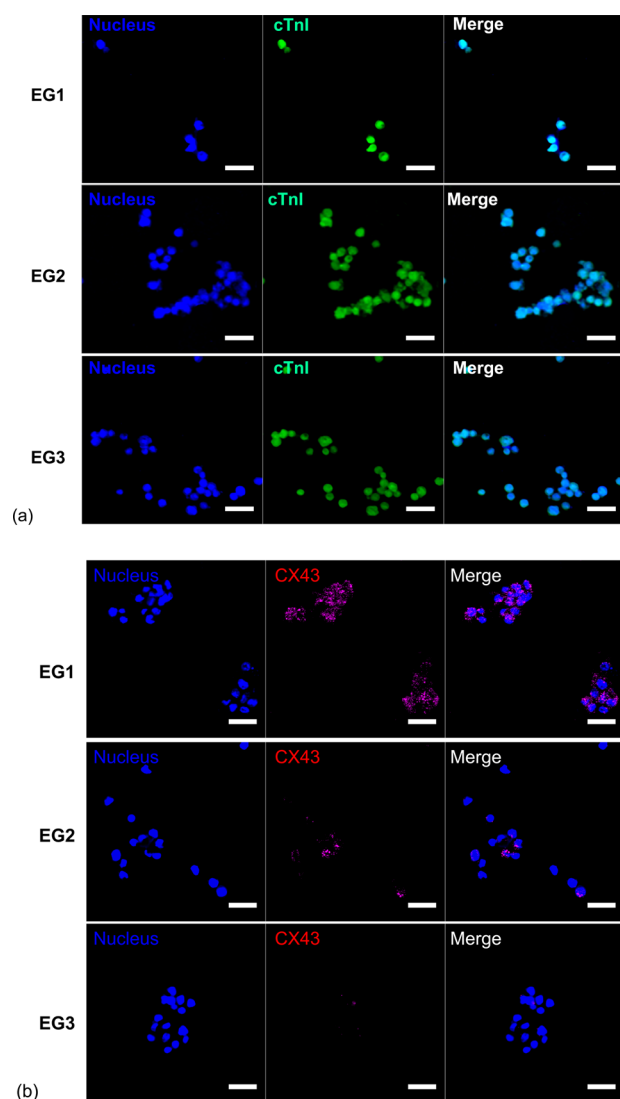


Figure 11. Immunohistochemical stainings of CDCs in hydrogels after 7 days of culture: (a) cTnI; (b) CX43. The scale bars are 50 μm .

side group increases. For PAA, the pK_a is ~ 6.3 ,⁴⁰ higher than that of acrylic acid (~ 3) and methacrylic acid (~ 4). Thus, PAA instead of acrylic acid and methacrylic acid was used as the pH-sensitive component in this report.

In the hydrogels, hydrophobic HEMA-*o*TMC and hydrophilic MA-PEG were used to provide additional adjustment for the LCST. It is known that the gelation of PNIPAAm-based hydrogels is the result of a balance between hydrophilic interaction with water and hydrophobic interaction between isopropyl groups.⁴⁴ The dissociation/association of PAA introduces the pH-dependent hydrophilic/hydrophobic interactions to the hydrogels. The components HEMA-*o*TMC and

MA-PEG can be used to further tune the range of pH sensitivity. At the same pH, the increase in the hydrophilic MA-PEG content increased the LCST (comparing EG1 to EG2 in Table 3). In contrast, an increase in the hydrophobic HEMA-*o*TMC content enhanced the hydrophobic interaction between polymer chains. As a result, the LCSTs of the hydrogels were significantly decreased (comparing EG3 and EG2 in Table 3). These results are consistent with the findings of Garben et al.⁴²

4.2. pH Dependence of the Hydrogel Degradation, Water Content, and Mechanical Properties.

The hydrogel degradation and water content were pH-dependent. All hydrogels showed significantly higher weight remaining in an acidic buffer (pH 6.5) than in a physiological buffer (pH 7.4) (Figure 7). During degradation, EG2 and EG3 hydrogels had higher water content at days 1, 7, and 14 in a pH 7.4 buffer than in a pH 6.5 buffer (Figure 7). The hydrogel degradation rate was dependent on the degree of protonation/deprotonation of the carboxyl groups in the hydrogels and hydrolysis of the carbonate side groups. Deprotonation of the carboxyl groups may lead to hydrogel dissolution, thus increasing the degradation rate. Because pH 7.4 is greater than the pK_a value of PAA, disassociation of PAA occurs at this pH. As a result, faster degradation is observed at this pH than at pH 6.5. In addition, deprotonation of the carboxyl groups increased the hydrogel hydrophilicity, as evidenced by higher water contents (Figure 7). This may accelerate the hydrolysis of *o*TMC side chains.

The mechanical properties of the hydrogels were dependent on the composition and pH. An increase in the MA-PEG ratio significantly decreased the hydrogel complex shear modulus (EG2 vs EG1, $p < 0.01$). This is possibly attributed to the PEG chains affecting the chain packing during the gelation process and decreasing the hydrophobic interactions. This result is consistent with our previous reports in which a decrease in the hydrophobic interaction significantly decreased the hydrogel elastic modulus.^{19,43,45} The hydrogels also demonstrated pH-responsive mechanical properties. Significantly higher complex shear moduli were observed in acidic buffers than in a pH 7.4 buffer at an initial 1 Hz (Table 4). Similar trend was found for EG2 and EG3 at 10% and 1 Hz except for EG1. It is possible that the relatively higher water content of EG1 facilitated chain alignment, leading to an increase of the complex shear modulus. All hydrogels demonstrated a shear-thinning behavior. This is in contrast to chemically cross-linked PEG hydrogels, which show a nearly frequency-independent Hookean-like behavior.^{46,47} The chemically cross-linked PEG hydrogels have stronger chemical covalent bonding between chains and thus may be more resistant to shear deformation than physically cross-linked PNIPAAm-based hydrogels, which have lower chain–chain interaction.

4.3. CDC Survival and Differentiation in Hydrogels.

The synthesized hydrogels exhibited good biocompatibility. When CDCs were encapsulated, the cells were able to survive

Table 4. Complex Shear Moduli of Hydrogels with Different Compositions under Different pH Values^a

gel	pH 6.5			pH 7.4		
	initial 1 Hz (Pa)	initial 10 Hz (Pa)	10% 1 Hz (Pa)	initial 1 Hz (Pa)	initial 10 Hz (Pa)	10% 1 Hz (Pa)
EG1	1418.7 \pm 39.8	1568.6 \pm 287.3	43.7 \pm 3.9	381.3 \pm 26.1	1702.2 \pm 115.1	251.2 \pm 12.0
EG2	580.5 \pm 14.4	788.7 \pm 45.8	101.8 \pm 4.4	24.8 \pm 4.1	189.3 \pm 37.7	21.4 \pm 0.4
EG3	1396.2 \pm 31.2	1242.0 \pm 46.8	106.5 \pm 4.1	41.3 \pm 5.2	319.0 \pm 78.0	31.4 \pm 9.5

^aThe hydrogels were formed at pH 6.5 and then incubated in pH 6.5 and 7.4 buffers for 24 h before the test.

during the 7-day culture period (Figures 8 and 9). The surviving cells also differentiated into cardiac lineage. At the gene level, CDCs in EG1 and EG3 hydrogels showed upregulated expressions of cTnT, MYH6, and CACNA1c (Figure 10). The highest expressions of these three markers were observed in the EG1 hydrogel. Immunofluorescent staining results demonstrated that more CDCs in the EG1 hydrogel than in the EG2 and EG3 hydrogels expressed CX43 (Figure 11). CDC differentiation in the hydrogels may be driven by the hydrogel mechanical and chemical properties. It is well-known that matrix mechanical properties stimulate stem-cell differentiation. For example, embryonic stem cells showed the greatest degree of cardiac differentiation in soft PEG hydrogels with a compressive modulus of 322 Pa.⁴⁸ In this report, the EG1 hydrogel had a similar modulus (381 Pa). This modulus is much greater than that in our previous report, where the optimal matrix modulus to trigger CDC differentiation was ~30 kPa (elastic modulus).¹⁴ It is possible that the optimal matrix modulus for CDC cardiac differentiation is in the range between 380 and 30 kPa, depending on the different differentiation and maturation stages of the cells. This is supported by the conclusions of Young et al., where a dynamic stiffening hydrogel with the modulus gradually increasing from 300 to 2 kPa is more optimal for maturation of cardiomyocytes than a statically compliant hydrogel.⁴⁹

5. CONCLUSIONS

In this work, a family of pH-sensitive and thermosensitive poly(NIPAAm-co-PAA-co-MA-PEG-co-HEMA-oTMC) hydrogels were synthesized by free-radical copolymerization. The hydrogels were injectable through catheters at 37 °C when the solution pH was adjusted to 8.0 and were able to form solid gels in an acidic (pH 6.5) environment similar to that of the infarcted heart tissue. The hydrogels showed pH-dependent properties. CDCs were able to survive and differentiate in the hydrogels during a 7-day culture period. These results demonstrated that the developed hydrogels can be attractive cell carriers for cardiac cell therapy. Besides cardiac application, the hydrogels may be used to deliver cells into other inflammatory soft tissues whose pH is typically 6–7.

AUTHOR INFORMATION

Corresponding Author

*Phone: 614-292-9743. E-mail: guan.21@osu.edu.

Author Contributions

‡These authors contributed equally to this work.

Notes

The authors declare no competing financial interest.

ACKNOWLEDGMENTS

This work was supported by the U.S. National Science Foundation (Grants 1006734 and 1160122), U.S. National Institutes for Health (Grant R01HL124122), American Heart Association (Grants 15GRNT25830058 and 13GRNT17150041), National Science Foundation of China (Grant 81471788), and Institute for Materials Research seed grant at The Ohio State University.

REFERENCES

(1) Dangas, G.; Badimon, J. J.; Collier, B. S.; Fallon, J. T.; Sharma, S. K.; Hayes, R. M.; Meraj, P.; Ambrose, J. A.; Marmur, J. D. Administration of Abciximab During Percutaneous Coronary Inter-

vention Reduces Both Ex Vivo Platelet Thrombus Formation and Fibrin Deposition: Implications for a Potential Anticoagulant Effect of Abciximab. *Arterioscler., Thromb., Vasc. Biol.* **1998**, *18* (8), 1342–1349.

(2) Hoffman, S. N.; TenBrook, J. A.; Wolf, M. P.; Pauker, S. G.; Salem, D. N.; Wong, J. B. A Meta-analysis of Randomized Controlled Trials Comparing Coronary Artery Bypass Graft with Percutaneous Transluminal Coronary Angioplasty: One- to Eight-year Outcomes. *J. Am. Coll. Cardiol.* **2003**, *41* (8), 1293–1304.

(3) San Juan, A.; Bala, M.; Hlawaty, H.; Portes, P.; Vranckx, R.; Feldman, L. J.; Letourneur, D. Development of a Functionalized Polymer for Stent Coating in the Arterial Delivery of Small Interfering RNA. *Biomacromolecules* **2009**, *10* (11), 3074–3080.

(4) Hoshino, K.; Kimura, T.; De Grand, A. M.; Yoneyama, R.; Kawase, Y.; Houser, S.; Ly, H. Q.; Kushibiki, T.; Furukawa, Y.; Ono, K.; Tabata, Y.; Frangioni, J. V.; Kita, T.; Hajjar, R. J.; Hayase, M. Three Catheter-based Strategies for Cardiac Delivery of Therapeutic Gelatin Microspheres. *Gene Ther.* **2006**, *13* (18), 1320–1327.

(5) Iwakura, A.; Fujita, M.; Kataoka, K.; Tambara, K.; Sakakibara, Y.; Komeda, M.; Tabata, Y. Intramyocardial Sustained Delivery of Basic Fibroblast Growth Factor Improves Angiogenesis and Ventricular Function in a Rat Infarct Model. *Heart Vessels* **2003**, *18* (2), 93–99.

(6) Martens, T. P.; Godier, A. F.; Parks, J. J.; Wan, L. Q.; Koeckert, M. S.; Eng, G. M.; Hudson, B. I.; Sherman, W.; Vunjak-Novakovic, G. Percutaneous Cell Delivery into the Heart using Hydrogels Polymerizing in situ. *Cell Transplant.* **2009**, *18* (3), 297–304.

(7) Qian, Q.; Qian, H.; Zhang, X.; Zhu, W.; Yan, Y.; Ye, S.; Peng, X.; Li, W.; Xu, Z.; Sun, L.; Xu, W. 5-Azacytidine Induces Cardiac Differentiation of Human Umbilical Cord-derived Mesenchymal Stem Cells by Activating Extracellular Regulated Kinase. *Stem Cells Dev.* **2012**, *21* (1), 67–75.

(8) Balana, B.; Nicoletti, C.; Zahanich, I.; Graf, E. M.; Christ, T.; Boxberger, S.; Ravens, U. 5-Azacytidine Induces Changes in Electrophysiological Properties of Human Mesenchymal Stem Cells. *Cell Res.* **2006**, *16* (12), 949–960.

(9) Bakunts, K.; Gillum, N.; Karabekian, Z.; Sarvazyan, N. Formation of Cardiac Fibers in Matrigel Matrix. *BioTechniques* **2008**, *44* (3), 341–348.

(10) Engler, A. J.; Carag-Krieger, C.; Johnson, C. P.; Raab, M.; Tang, H. Y.; Speicher, D. W.; Sanger, J. W.; Sanger, J. M.; Discher, D. E. Embryonic Cardiomyocytes Beat Best on a Matrix with Heart-like Elasticity: Scar-like Rigidity Inhibits Beating. *J. Cell Sci.* **2008**, *121* (22), 3794–3802.

(11) Kehat, I.; Kenyagin-Karsenti, D.; Snir, M.; Segev, H.; Amit, M.; Gepstein, A.; Livne, E.; Binah, O.; Itskovitz-Eldor, J.; Gepstein, L. Human Embryonic Stem Cells Can Differentiate into Myocytes with Structural and Functional Properties of Cardiomyocytes. *J. Clin. Invest.* **2001**, *108* (3), 407–414.

(12) Foldes, G.; Mioulane, M.; Chahine, M. N.; Schneider, M. D.; Harding, S. E. 29 Human Induced Pluripotent Stem Cell-derived Cardiomyocytes Serve as in Vitro Model of Cardiac Hypertrophy. *Heart* **2011**, *97* (20), e7.

(13) Davis, D. R.; Zhang, Y.; Smith, R. R.; Cheng, K.; Terrovitis, J.; Malliaras, K.; Li, T. S.; White, A.; Makkar, R.; Marban, E. Validation of the Cardiosphere Method to Culture Cardiac Progenitor Cells from Myocardial Tissue. *PLoS One* **2009**, *4* (9), e7195.

(14) Li, Z.; Guo, X.; Matsushita, S.; Guan, J. Differentiation of Cardiosphere-derived Cells into a Mature Cardiac Lineage using Biodegradable Poly(N-isopropylacrylamide) Hydrogels. *Biomaterials* **2011**, *32* (12), 3220–3232.

(15) Davis, D. R.; Kizana, E.; Terrovitis, J.; Barth, A. S.; Zhang, Y.; Smith, R. R.; Miale, J.; Marban, E. Isolation and Expansion of Functionally-competent Cardiac Progenitor Cells Directly from Heart Biopsies. *J. Mol. Cell. Cardiol.* **2010**, *49* (2), 312–321.

(16) Perin, E. C.; Tian, M.; Marini, F. C., 3rd; Silva, G. V.; Zheng, Y.; Baimbridge, F.; Quan, X.; Fernandes, M. R.; Gahremanpour, A.; Young, D.; Paolillo, V.; Mukhopadhyay, U.; Borne, A. T.; Uthamanthil, R.; Brammer, D.; Jackson, J.; Decker, W. K.; Najjar, A. M.; Thomas, M. W.; Volgin, A.; Rabinovich, B.; Soghomonyan, S.; Jeong, H. J.; Rios, J. M.; Steiner, D.; Robinson, S.; Mawlawi, O.; Pan, T.; Stafford, J.

Kundra, V.; Li, C.; Alauddin, M. M.; Willerson, J. T.; Shpall, E.; Gelovani, J. G. Imaging Long-term Fate of Intramyocardially Implanted Mesenchymal Stem Cells in a Porcine Myocardial Infarction Model. *PLoS One* **2011**, *6* (9), e22949.

(17) Williams, A. R.; Trachtenberg, B.; Velazquez, D. L.; McNiece, I.; Altman, P.; Rouy, D.; Mendizabal, A. M.; Pattany, P. M.; Lopera, G. A.; Fishman, J.; Zambrano, J. P.; Heldman, A. W.; Hare, J. M. Intramyocardial Stem Cell Injection in Patients with Ischemic Cardiomyopathy: Functional Recovery and Reverse Remodeling. *Circ. Res.* **2011**, *108* (7), 792–796.

(18) Huang, W.; Wang, T.; Zhang, D.; Zhao, T.; Dai, B.; Ashraf, A.; Wang, X.; Xu, M.; Millard, R. W.; Fan, G. C.; Ashraf, M.; Yu, X. Y.; Wang, Y. Mesenchymal Stem Cells Overexpressing CXCR4 Attenuate Remodeling of Postmyocardial Infarction by Releasing Matrix Metalloproteinase-9. *Stem Cells Dev.* **2012**, *21* (5), 778–789.

(19) Li, Z.; Wang, F.; Roy, S.; Sen, C. K.; Guan, J. Injectable, Highly Flexible, and Thermosensitive Hydrogels Capable of Delivering Superoxide Dismutase. *Biomacromolecules* **2009**, *10* (12), 3306–3316.

(20) Xu, Y.; Fu, M.; Li, Z.; Fan, Z.; Li, X.; Liu, Y.; Anderson, P. M.; Xie, X.; Liu, Z.; Guan, J. A Prosurvival and Proangiogenic Stem Cell Delivery System to Promote Ischemic Limb Regeneration. *Acta Biomater.* **2016**, *31* (15), 99.

(21) Li, Z.; Guo, X.; Guan, J. A Thermosensitive Hydrogel Capable of Releasing bFGF for Enhanced Differentiation of Mesenchymal Stem Cell into Cardiomyocyte-like Cells under Ischemic Conditions. *Biomacromolecules* **2012**, *13* (6), 1956–1964.

(22) Li, Z.; Guo, X.; Guan, J. An Oxygen Release System to Augment Cardiac Progenitor Cell Survival and Differentiation under Hypoxic Condition. *Biomaterials* **2012**, *33* (25), 5914–5923.

(23) Thornton, A. J.; Alsberg, E.; Albertelli, M.; Mooney, D. J. Shape-defining Scaffolds for Minimally Invasive Tissue Engineering. *Transplantation* **2004**, *77* (12), 1798–1803.

(24) Tyagi, P.; Li, Z.; Chancellor, M.; De Groat, W. C.; Yoshimura, N.; Huang, L. Sustained intravesical drug delivery using thermosensitive hydrogel. *Pharm. Res.* **2004**, *21* (5), 832–837.

(25) Thompson, C. A.; Nasser, B. A.; Makower, J.; Houser, S.; McGarry, M.; Lamson, T.; Pomerantseva, I.; Chang, J. Y.; Gold, H. K.; Vacanti, J. P.; Oesterle, S. N. Percutaneous Transvenous Cellular Cardiomyoplasty. A Novel Nonsurgical Approach for Myocardial Cell Transplantation. *J. Am. Coll. Cardiol.* **2003**, *41* (11), 1964–1971.

(26) Shim, W. S.; Yoo, J. S.; Bae, Y. H.; Lee, D. S. Novel Injectable pH and Temperature Sensitive Block Copolymer Hydrogel. *Biomacromolecules* **2005**, *6* (6), 2930–2934.

(27) Cohen, M. V.; Yang, X. M.; Downey, J. M. The pH Hypothesis of Postconditioning: Staccato Reperfusion Reintroduces Oxygen and Perpetuates Myocardial Acidosis. *Circulation* **2007**, *115* (14), 1895–1903.

(28) Lemasters, J. J.; Bond, J. M.; Chacon, E.; Harper, I. S.; Kaplan, S. H.; Ohata, H.; Trollinger, D. R.; Herman, B.; Cascio, W. E. The pH Paradox in Ischemia-reperfusion Injury to Cardiac Myocytes. *Exs.* **1996**, *76*, 99–114.

(29) Strehin, I.; Nahas, Z.; Arora, K.; Nguyen, T.; Elisseeff, J. A Versatile pH Sensitive Chondroitin Sulfate-PEG Tissue Adhesive and Hydrogel. *Biomaterials* **2010**, *31* (10), 2788–2797.

(30) Schmaljohann, D. Thermo- and pH-responsive Polymers in Drug Delivery. *Adv. Drug Delivery Rev.* **2006**, *58* (15), 1655–1670.

(31) Frutos, G.; Prior-Cabanillas, A.; Paris, R.; Quijada-Garrido, I. A Novel Controlled Drug Delivery System Based on pH-responsive Hydrogels Included in Soft Gelatin Capsules. *Acta Biomater.* **2010**, *6* (12), 4650–4656.

(32) Wu, D. Q.; Sun, Y. X.; Xu, X. D.; Cheng, S. X.; Zhang, X. Z.; Zhuo, R. X. Biodegradable and pH-sensitive Hydrogels for Cell Encapsulation and Controlled Drug Release. *Biomacromolecules* **2008**, *9* (4), 1155–1162.

(33) Yang, Y. Q.; Zheng, L. S.; Guo, X. D.; Qian, Y.; Zhang, L. J. pH-Sensitive Micelles Self-assembled from Amphiphilic Copolymer Brush for Delivery of Poorly Water-soluble Drugs. *Biomacromolecules* **2011**, *12* (1), 116–122.

(34) Shim, W. S.; Kim, S. W.; Lee, D. S. Sulfonamide-based pH- and Temperature-sensitive Biodegradable Block Copolymer Hydrogels. *Biomacromolecules* **2006**, *7* (6), 1935–1941.

(35) Huynh, D. P.; Nguyen, M. K.; Pi, B. S.; Kim, M. S.; Chae, S. Y.; Lee, K. C.; Kim, B. S.; Kim, S. W.; Lee, D. S. Functionalized Injectable Hydrogels for Controlled Insulin Delivery. *Biomaterials* **2008**, *29* (16), 2527–2534.

(36) Huynh, C. T.; Nguyen, M. K.; Lee, D. S. Biodegradable pH/temperature-sensitive Oligo(beta-amino ester urethane) Hydrogels for Controlled Release of Doxorubicin. *Acta Biomater.* **2011**, *7* (8), 3123–3130.

(37) Wang, C.; Javadi, A.; Ghaffari, M.; Gong, S. A pH-sensitive Molecularly Imprinted Nanospheres/hydrogel Composite as a Coating for Implantable Biosensors. *Biomaterials* **2010**, *31* (18), 4944–4951.

(38) Yoshikawa, H. Y.; Rossetti, F. F.; Kaufmann, S.; Kaindl, T.; Madsen, J.; Engel, U.; Lewis, A. L.; Armes, S. P.; Tanaka, M. Quantitative Evaluation of Mechanosensing of Cells on Dynamically Tunable Hydrogels. *J. Am. Chem. Soc.* **2011**, *133* (5), 1367–1374.

(39) Van Butsele, K.; Morille, M.; Passirani, C.; Legras, P.; Benoit, J. P.; Varshney, S. K.; Jerome, R.; Jerome, C. Stealth Properties of Poly(ethylene oxide)-based Triblock Copolymer Micelles: a Prerequisite for a pH-triggered Targeting System. *Acta Biomater.* **2011**, *7* (10), 3700–7.

(40) Murthy, N.; Robichaud, J. R.; Tirrell, D. A.; Stayton, P. S.; Hoffman, A. S. The Design and Synthesis of Polymers for Eukaryotic Membrane Disruption. *J. Controlled Release* **1999**, *61* (1–2), 137–143.

(41) Garbern, J. C.; Hoffman, A. S.; Stayton, P. S. Injectable pH- and Temperature-responsive Poly(N-isopropylacrylamide-co-propylacrylic acid) Copolymers for Delivery of Angiogenic Growth Factors. *Biomacromolecules* **2010**, *11* (7), 1833–1839.

(42) Garbern, J. C.; Minami, E.; Stayton, P. S.; Murry, C. E. Delivery of Basic Fibroblast Growth Factor with a pH-responsive, Injectable Hydrogel to Improve Angiogenesis in Infarcted Myocardium. *Biomaterials* **2011**, *32* (9), 2407–2416.

(43) Wang, F.; Li, Z.; Khan, M.; Tamama, K.; Kuppusamy, P.; Wagner, W. R.; Sen, C. K.; Guan, J. Injectable, Rapid Gelling and Highly Flexible Hydrogel Composites as Growth Factor and Cell Carriers. *Acta Biomater.* **2010**, *6* (6), 1978–1991.

(44) Ahmed, Z.; Gooding, E. A.; Pimenov, K. V.; Wang, L.; Asher, S. A. UV Resonance Raman Determination of Molecular Mechanism of Poly(N-isopropylacrylamide) Volume Phase Transition. *J. Phys. Chem. B* **2009**, *113* (13), 4248–4256.

(45) Guan, J.; Hong, Y.; Ma, Z.; Wagner, W. R. Protein-reactive, Thermoresponsive Copolymers with High Flexibility and Biodegradability. *Biomacromolecules* **2008**, *9* (4), 1283–92.

(46) Lin, C. C.; Metters, A. T.; Anseth, K. S. Functional PEG-peptide Hydrogels to Modulate Local Inflammation Induced by the Pro-inflammatory Cytokine TNFalpha. *Biomaterials* **2009**, *30* (28), 4907–4914.

(47) Weber, L. M.; He, J.; Bradley, B.; Haskins, K.; Anseth, K. S. PEG-based Hydrogels as an in Vitro Encapsulation Platform for Testing Controlled Beta-cell Microenvironments. *Acta Biomater.* **2006**, *2* (1), 1–8.

(48) Kraehenbuehl, T. P.; Zammaretti, P.; Van der Vlies, A. J.; Schoenmakers, R. G.; Lutolf, M. P.; Jaconi, M. E.; Hubbell, J. A. Three-dimensional Extracellular Matrix-directed Cardioprogenitor Differentiation: Systematic Modulation of a Synthetic Cell-responsive PEG-hydrogel. *Biomaterials* **2008**, *29* (18), 2757–2766.

(49) Young, J. L.; Engler, A. J. Hydrogels with Time-dependent Material Properties Enhance Cardiomyocyte Differentiation in Vitro. *Biomaterials* **2011**, *32* (4), 1002–1009.